Proceedings of the 28th IEEE
EMBS Annual International Conference
New York City, USA, Aug 30-Sept 3, 2006

3D Statistical Shape Models of Patella for Sex Classification

Mohamed Mahfouz, Ahmed Badawi, Brandon Merkl, Emam E. Abdel Fatah, Emily Pritchard, Katherine Kesler, Megan Moore, Richard Jantz

***Abstract*—. This paper proposes a new sex classification method from patellae using a novel automated feature extraction technique. A dataset of 228 patellae (95 females and 133 males) was collected and CT scanned. After the CT data was segmented, a set of features was automatically extracted, normalized, and ranked. These features include geometric features, moments, principal axes, and principal components. A feature vector of 45 dimensions for each subject was then constructed. A set of statistical and supervised neural network classification methods were used to classify the patellar feature vectors according to sex. Different classification methods were compared. Classification success ranged from 83.77% average classification rate with labeling using fuzzy C-Means method (FCM), to 90.3% for linear discriminant function (LDF) analysis. We obtained results of 96.02% and 93.51% training and testing classification rates (respectively) using feed-forward backpropagation Neural Networks (NN). These promising results encourage the usage of this method in forensic anthropology for identifying the sex from incomplete skeletons containing at least one patella.**

I. Introduction

Sex classification is one of the major challenges for the forensic anthropologist within a medical-legal context. Sex classification is called sex determination by forensic anthropologists and the medical/legal communities in general. Sex determination is one of the essential steps in personal identification of an individual from skeletal remains, often looking at bone morphology to determine the sex (morphological sexing). The estimation of sex is more reliable if the complete skeleton is available for analysis, but in forensic cases human skeletal remains are often incomplete or damaged. The pelvic bone and skull are the first choices for morphological sexing if not recovered in fragmentary states. If pelvic bones and skull are recovered in a fragmentary state, other bones such as the patella can be used. For many years, sex determination has been studied from skeletal remains either for archaeological purposes [1] or forensic purposes [2]. Morphological and metrical features of some bones that display sexual differences have been described [2]. These sexual differences include the pelvis [3–6], the cranium [7–13], bones of the upper limb [14–15] and lower limb [16–23], and some fragments of bones [24–29]. Recently, there has been an increased interest in the use of statistical methods in sex determination. The most commonly used statistical method in analyzing this sex determination problem is discriminant function analysis [30], which has been described by [16–17]. Most bones have been subjected to discriminant function analysis [16] but not much literature has been found on the usefulness of measurements of the patella in the determination of sex using this method. Iscan [39] summarized the importance of sex differences and sex determination in forensic anthropology and explained the current research in sexual variation and body size.

Mohamed Mahfouz, Ahmed Badawi, Brandon Merkl, Emam E. Abdel Fatah, Emily Pritchard, Katherine Kesler are with Biomedical Engineering Department, University of Tennessee, Knoxville.

Megan Moore, Richard Jantz are with Anthropology Department, University of Tennessee, Knoxville. Correspondence to: mmahfouz@utk.edu.

II. Previous Work

The patella is a small compact bone that develops within the quadriceps femoris muscle tendon and does not undergo many postmortem changes and therefore can be retrieved complete and can be used for sex estimation [32]. It is a roughly triangular, flat bone that has an articulating facet for the distal anterior end of the femur. Since the shape and the size of the patella relies on the strength of the muscle mass, then stronger muscle masses could alter the shape and size of patella. Males have a more robust muscle build compared to females, it would be expected that some measurements of the patella would display sexual dimorphism [37].

Recent work has explored sexual dimorphism in the patella as a possible method for sex determination of partial or fragmentary human remains. Most research groups relied on the measurements of six geodesic parameters. These measurements are maximum height, maximum width, maximum thickness, height of articular facet, medial articular facet breadth, and lateral articular facet breadth. Wendi O'Connor [38] demonstrated a statistically significant dimorphism in patellae measurements collected from the Terry Collection and radiographs of college students and had an accuracy result of 82.5% in classification of females and 78.6% classification of males. Introna et al. [32] also established that patellar maximum width and thickness resulted in high accuracy rate of 83.8% in determining sex using multivariate discriminant analysis. Taterk et al. [35] reanalyzed the O'Connor's work and reported an accuracy of 67%-80% using a discriminant function, using single patella or both. Due to their low accuracies, they recommended utilizing the patella as a sex determinant in conjunction with other diagnostic skeletal elements. More recent studies include, Bidmos et al. [34] who analyzed the problem using six measurements and

reported an overall accuracy of 83% using a linear discriminant analysis. Subsequently, Ariane Kemkes-Grottenthaler [36] reported an accuracy of 85%; however, when the sample size was taken into consideration, results dropped to 78%. The third paper by Dayal et al. [37] analyzed this problem using six measurements with classification result of 85%.

Iscan [39] stated that the patella seems to be the most omitted bone in forensic anthropology despite the fact that some sexual differences are expected to exist as it plays a significant role in the knee joint and since the femur and tibia are highly dimorphic. Most researchers who used patellae for sex determination relied only on the basic geodesic measurements from the patella such as maximum height, width, thickness, and height of the articular facets. Also, most of the previous work in patellae used these geodesic measurements only to drive linear discriminant classification functions to separate the feature space; however, none of these groups investigated the use of other non-geodesic features as well as investigating nonlinear classification methods such as the ones proposed in this paper.

In the last 20 years, applications of nonlinear classification methods such as neural networks and fuzzy logic rule-based techniques have been used for the computerized diagnosis of diseases with medical imaging. We have previously analyzed the problem of quantitative liver tissue characterization using neural networks and fuzzy logic [40-41], bladder outlet obstruction computerized diagnosis [42-43], and automated chromosome classification [44]. In this paper we propose a new method for sex determination which extracts more categories of features other than the geodesic measurements and analyzes the classification problem in a nonlinear approach using neural networks.

III. Methods and Materials

A. Data Acquisition

A data set of 228 patellae (95 females and 133 males) for recent North American populations was CT scanned in an arrangement as shown in Figures 1 and 2.

Figure 1: *In vitro* patellae prepared for CT scanning

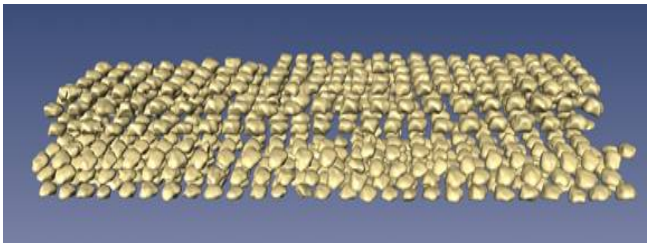

Figure 2: Segmented patellae

Only normal patellae were included in this study; patellae with severe osteophytes and other abnormalities were specifically excluded. The majority of the patellae (210 out of 228) came from the William M. Bass Donated Skeletal Collection from the University of Tennessee Anthropology Department. These dry bones were scanned using a GE Lightspeed 16 Slice computed tomography scanner. Patellae were scanned using 0.625x0.625x0.625 mm cubic voxels. Eighteen patellae came from live patient and cadaveric *in vivo* CT data with a maximum voxel size of 0.488x0.488x1.5 mm. All patellae were segmented manually. After segmentation, triangular surface meshes were generated using Amira (Mercury Computer Sys., San Diego). Models were created with 2000 - 7000 triangulated faces, which was chosen to adequately represent bone morphology while minimizing data storage constraints.

B. Patella Atlas Construction

Comparing all of the bone models in our dataset, we chose a bone model with average shape characteristics to act as a template mesh. The points in the template mesh (N=2502 vertices) are then matched to corresponding points in all of the other training models. This ensures that all of the bones have the same number of vertices and the same triangular connectivity, a requirement of Principal Components Analysis (PCA). We use a series of registration and warping techniques to pick corresponding points on all the other bone models in the training set. The process of picking point correspondences on new models to be added to the atlas is "non-trivial" [45]. The matching algorithm that follows uses several well-known techniques of computer vision as well as our novel contribution for final surface alignment.

First, the centroids of the template mesh and the new mesh are aligned and the template mesh is pre-scaled to match the bounding box dimensions of the template model with that of the new mesh. Second, a rigid alignment of the template mesh to the new mesh is performed using a standard vertex-to-vertex Iterative Closest Point (ICP) algorithm [46]. Third, after rigid alignment we perform a general affine transformation without iteration. This method is applied to align the template mesh to the new mesh that uses 12 degrees of freedom (DOF) (rotations, translations, scaling, and shear). After the affine transformation step, the template and new model have reached the limits of linear transformation, but portions of the models still remain significantly distant. The goal of final surface-to-surface matching is to create new points on the surface of the new

model, which will have similar local spatial characteristics as the template model.

To reduce this misalignment, we have previously developed a novel non-linear iterative warping approach, which we term Mutual Correspondence Warping (MCW) [47]. In this method, point correspondences are picked in both directions. For every iteration of the algorithm, the closest vertex-to-vertex correspondences are found from the template to the new model as before, but now we also find the correspondences from the new model to the template model. Using both of these point correspondences, points on the template mesh are moved toward locations on the new mesh using a non-symmetric weighting of the vectors of correspondence.

$$P^{new} = P^{old} + \left(C_1\overline{V} - C_2\overline{U}\right). \quad (1)$$

where P represents points on the template model, V is the correspondence vector that points from the template to the new model. U is the correspondence vector that points from the new to the template model. The vector *V* will have a one-to-one relationship with template points, but the *U* vector initially can have many-to-one or null-to-one relationships with template points. Preceding the evaluation of (1) in cases of many-to-one relationships, we use the mean of the many correspondence vectors. The null-to-one relationships create discontinuities in the model surface and thus a smoothing step is desired.

A subroutine consisting of an iterative smoothing algorithm is applied to the now-deformed template mesh. This smoothing algorithm seeks to average the size of adjacent triangles on the template mesh, eliminating discontinuities. At the beginning of MCW, the smoothing algorithm uses the actual areas of the surrounding triangles to dictate the smoothing vector applied to each point. Effectually, this aids in removing outlying points with large triangles. At the beginning of the process, the template mesh makes large steps and larger smoothing is required. Toward the end of the process, the smoothing vector applied is normalized by the total area of the surrounding triangles; which allows for greater expansion of the template mesh into areas of high curvature.

After this procedure has been performed on all the patellae, Principal Components Analysis (PCA) is performed by first computing the mean patella shape (μ) by averaging the corresponding points across all models. The data matrix is constructed

$$m_i = \left(\left(x_1^i \; y_1^i \; z_1^i \cdots x_N^i \; y_N^i \; z_N^i\right) - \mu\right)^T \quad (2)$$

$$M = \left(m_1 \mid \cdots \mid m_B\right) \quad (3)$$

$$[USV^T] = svd(M) \quad (4)$$

where m_i is the feature vector associated with each *B* models, the number of points per model is *N*, the Singular Value Decomposition is represented with *SVD(),* and the eigenvectors are taken as the leftmost columns of ***U***, given that the singular values along the diagonal of ***S*** are sorted from largest to smallest. The eigenvectors, which are orthogonal, define a new set of coordinates with reduced dimensionality with respect to *N* when the original features (m_i) are projected onto the eigenvalues scaled by the square root of the eigenvalues. These PCA coordinates are recorded for each model and are later used for classification.

The template mesh frame coordinate frame is defined as follows: the centroid of the model is at the origin, the +x axis points in the direction of the most medial aspect of the patella, the +y axis points anteriorly, and the +z axis is mutually perpendicular to both of these axes and points roughly in a superior direction.

C. Geometric Feature Extraction

Following the atlas construction and alignment steps outlined above, all the patellae models now lie in the same coordinate frame and have homologous points and faces. In this coordinate frame, six points are found to be the maximum and minimum values for the coordinates x, y, and z respectively. Using these points, three features are generated that represent the Euclidean distance between pairs of points in each coordinate direction. This yields three measures of maximum mediolateral (ML) width, maximum anteroposterior (AP) depth, and superoinferior (SI) height. Additionally, the six points are used to construct a bounding box around the patella, which is used to extract three features describing bounding box width (BBML), bounding box depth (BBAP), and bounding box height (BBSI).

Three vectors were defined forming a triangle; one that pointed from the most lateral aspect to the most medial aspect, one that pointed from the most lateral aspect to the most posterior aspect of the patella, as well as one that connected the most posterior aspect with the most medial aspect (Fig. 3). This triangle was projected on a plane perpendicular to the z-axis transforming the vectors into two-dimensions (2D). The lengths of the sides of the triangle were recorded as features. Also the angles relative to the x-axis were measured relative to the lateral-posterior vector (α) as well as measured relative to the ML vector (β). The angle (γ) is defined between the lateral-posterior and the medial-posterior vectors and is shown along with the other 2D measurements in Figure 3. In addition to these features several other angular measures were defined. The angle formed by the medial, inferior, and lateral points (MIL) measures the degree of pointed-ness of the patellar nose. Additionally, the superior shelf angle (SSA) measures the angle of slope of the superior-anterior facet relative to the +z-axis. Finally, using two patches of corresponding points, one on the medial-posterior articulating facet and one on the lateral-posterior articulating facet, an orthogonal distance regression plane is fit to each patch of points; the relative angle between these two planes is recorded as the posterior facet angle (PFA). A second version of this angle is reported as PFN, and represents the angle PFA projected on the xy-plane. This measure was developed to measure the

ML angle between the facets without regard to out-of-plane differences in the SI direction.

Another set of features were developed by computing the model moment of inertia around various axes. The moments of inertia calculated in these measures are only point-wise measures that only approximate the inertia of the surface of the model. The first three axes were computed in the direction of the Cartesian coordinates, but passing through the models centroid. These three axes yield measurements I_{xx}, I_{yy}, and I_{zz}. Next, the inertias for the three perpendicular principal axes were developed. These inertias were recorded as I_1, I_2, and I_3. Also, thin disks consisting of exactly 50 points were found about the circumference of the model at the midpoint of the bounding box for each Cartesian direction. The moments of inertia for these 50 points are recorded as I_x, I_y, and I_z. Table 1 lists the total categories of extracted features (25 features).

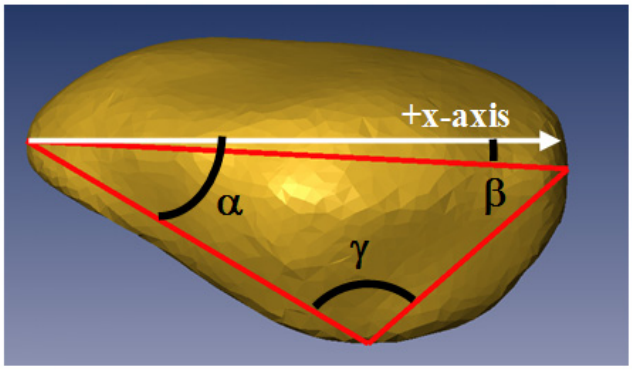

Figure 3: Patella viewed from the inferior, showing the various 2D measurements: 2D ML width (ML2D), 2D lateral-posterior length (LP2D), 2D medial-posterior length (MP2D, and angle measures α,β and γ.

Table 1: Total categories of extracted features (25 features).

Geometric Category	Moment Category	Angular Category
BBML	I_{xx}‡	α‡
BBSI‡	I_{yy}‡	β‡
BBAP‡	I_{zz} ‡	γ‡
ML‡	I_1‡	PFN
SI‡	I_2‡	PFA
AP‡	I_3‡	SSA
ML2D‡	I_x	MIL
LP2D‡	I_y	-
MP2D‡	I_z	-

Features denoted with a (‡) were then normalized by the ML width, BBML, and were added to the total list of feature vectors (17 additional features). Extra functional midterm features (3 additional features) were generated and added to the feature vector as shown in Table 2.

Table 2: Features generated by midterms

$I_x * I_y * I_z$
BBAP*I_x
BBAP* I_y

The overall feature vector dimensionality is 45 after adding the normalized features to the list of vectors. Features ranking was performed in order to find the most significant features that partitions the feature space. A Fuzzy C-Means algorithm as an unsupervised method for clustering was first performed in order to cluster data. A linear discriminant classification was also performed and finally a neural network classification was performed as nonlinear classification method. The results for each classification method are discussed in the results section.

IV. Results

A. Descriptive Statistical Results for All Features

Table 3 shows the statistical values presented for both sexes.

Table 3. Statistical results for both sexes.

	Female		*Male*		
Feature	Mean	STD	Mean	STD	t-test
$I_x * I_y * I_z$	8.2E+6	3.7E+6	1.70E+7	7.0E+6	<0.01
I_{yy}	4104.03	498.65	5270.74	743.03	<0.01
SI/BBML	0.99	0.06	0.99	0.07	0.62
I_{zz}	6117.16	797.53	7933.81	1024.93	<0.01
α/BBML	-7.12	1.17	-6.15	1.17	<0.01
I_{xx}	3835.34	528.72	4858.11	593.79	<0.01
PFN	52.44	7.41	48.75	8.10	<0.01
I_x	171.29	26.18	218.94	29.56	<0.01
PFA	52.21	7.03	49.03	7.01	<0.01
BBSI	4.04	0.33	4.60	0.31	<0.01
BBML	4.08	0.29	4.67	0.38	<0.01
BBAP	2.79	0.27	3.19	0.38	<0.01

B. Feature Ranking and Reduced Set of Features

Features were ranked for its maximum significance in classification using Fischer analysis. In order to select the most significance features subset, we calculated a scalar, Fisher's discriminate ratio (FDR), for each feature that corresponds to its power of separation with respect to sex. Then the whole features can be ranked according to their power of separation, and the desired number of features can be selected. Table 5 shows the highest significant features that were used to drive different classification methods.

Table 4: Shows the highest ranked 9 features based on FDR values.

Feature	*FDR Value*
$I_x * I_y * I_z$	36.33
I_{yy}	17.07
SI/BBML	11.17
I_{zz}	10.2
α/BBML	9.27
I_{xx}	7.6
PFN	6.29
I_x	3.03
PFA	2.78

C. Fuzzy C-Means clustering

Table 5 shows the results from FCM as a confusion matrix. The overall correct classification accuracy was found to be 83.77%.

Table 5: Results of confusion matrix using FCM clustering on the geometric features

	Predicted		
Actual	Female	Male	Total
Female	89	6	95
Male	31	102	133
Total	120	108	228

D. Linear Discriminant Classification

Table 6 shows the results from of linear discriminant classification as a confusion matrix using the highest 9 significant features. The overall correct classification accuracy was found to be 90.3%.

Table 6: Results of confusion matrix using LDC on the geometric features

	Predicted		
Actual	Female	Male	Total
Female	80	15	95
Male	7	126	133
Total	87	141	228

Additional testing was performed on only the PCA features using LDC. The resulting confusion matrix is outlined below in Table 7. The overall accuracy for this method was 91.7%.

Table 7: Results of confusion matrix using LDC on the PCA features

	Predicted		
Actual	Female	Male	Total
Female	90	5	95
Male	14	119	133
Total	104	124	228

E. *Neural Network Classification*

A standard feed-forward back propagation neural network algorithm was used for classification. 151 patella cases were used to train the network and 77 patella cases to test the network. Input/Hidden/Output (I/H/O) size was set to 45/60/2. Epoch size was 10000. MSE was 0.04. Learning factor (Alpha) was 0.5, Momentum term was 0.8, with a tan-sigmoidal functional activation. Tables 8 and 9 show the results from NN classification as a confusion matrix using all the 45 features; utilizing the ability of the neural network to rank the features vector by adjusting the weights of the highest significant features. The overall correct classification accuracy was found to be 93.51% for testing and 96.02% for training.

Table 8: Training results of confusion matrix using NN on the geometric features

	Predicted		
Actual	Female	Male	Total
Female	61	3	64
Male	3	84	87
Total	64	87	151

Table 9: Testing results of confusion matrix using NN on the geometric features

	Predicted		
Actual	Females	Males	Total
Female	28	3	31
Male	2	44	46
Total	30	47	77

Additional testing was performed on only the PCA features using NN. The NN using the PCA features did not perform as well as the NN using the geometric features comparing both in the testing phase. The training confusion matrix is outlined below in Table 10 and the testing confusion matrix is shown in Table 11. The overall accuracy for this method was 90.9%.

Table 10: Training results of confusion matrix using NN on the PCA features

	Predicted		
Actual	Female	Male	Total
Female	64	1	65
Male	0	86	86
Total	64	87	151

Table 11: Testing results of confusion matrix using NN on the PCA features

	Predicted		
Actual	Females	Males	Total
Female	28	2	30
Male	5	42	47
Total	33	44	77

V. Conclusion

In our study, we obtained a classification of 93.51% in sex determination using the patella, compared to 85% found in our literature survey [36]. We attribute our good results to a number of factors. First, most of the research groups in the medical, legal, and forensic anthropology fields rely on manual measurements using calipers, while we used 3D CT imaging for automating the extraction of measurements. Second, we extracted from the segmented patellae multiple categories such as geometric features, moments, and principal axes. By adding new features to the feature vector we increased the accuracy of the LDA to 90.3% which is an improvement over existing published methodologies. In addition we used a NN which increased the classification accuracy to 93.51%. Our novel analysis offers a new method for using only the patella for sex determination in the case where the entire skeletal remains are not found or are damaged. These results agree with the recent four publications in the literature [34-37]. This analysis is extremely useful in forensic and medical applications.

References

[1] Schutkowski H "Sex determination of infant and juvenile skeletons I: morphognostic features", Am J Phys Anthropol 1993;90:199–205.

[2] Scheuer L. "A blind test of mandibular morphology for sexing mandibles in the first few years of life", Am J Phys Anthropol 2002;119:189–91.

[3] Schulter–Ellis FP, Schmidt DJ, Hayek LA, Craig J. "Determination of sex with a discriminant analysis of new pelvic bone measurements: Part I",
J Forensic Sci 1983;28:169–80.

[4] Luo Y. "Sex determination from the pubis by discriminant function analysis", Forensic Sci Int 1995;74:89–98.

[5] Murphy AMC. "The acetabulum: sex assessment of prehistoric new Zealand polynesian innominates", Forensic Sci Int 2000;108:39–43.

[6] Bruzek J. "A method for visual determination of sex, using the human hip Bone", Am J Phys Anthropol 2002;117:157–68.

[7] Kajanoja P. "Sex determination of Finnish crania by discriminant function analysis", Am J Phys Anthropol 1966;24:29–34.

[8] De Villiers H. "Sexual dimorphism of the skull of the South African Bantu–speaking Negro", S Afr J Sci 1968;64:118–24.

[9] Kieser JA, Groeneveld HT. "Multivariate sexing of the human viscerocranium", J Forensic Odontostomatol 1986;4:41–6.

[10] Holland TD. "Sex determination of fragmentary crania by analysis of the cranial base", Am J Phys Anthropol 1986;70:203–8.

[11] Loth SR, Henneberg M. "Mandibular ramus flexure: A new morphologic indicator of sexual dimorphism in the human skeleton", Am J Phys Anthropol 1996;99:473–85.

[12] Steyn M, ˙Iscan MY. "Sexual dimorphism in the crania and mandibles of South African whites", Forensic Sci Int 1998;98:9–16.

[13] Gulekon IN, Turgut HB. "The external occipital protuberance: can it be used as a criterion in the determination of sex?", J Forensic Sci 2003;48:513–6.

[14] Iscan MY, Loth SR, King CA, Shihai D, Yoshino M. "Sexual dimorphism in the humerus: A comparative analysis of Chinese, Japanese and Thais", Forensic Sci Int 1998;98:17–29.

[15] SteynM, ˙Iscan MY. "Osteometric variation in the humerus: sexual dimorphism in South Africans", Forensic Sci Int 1999;106:77–85.

[16] Bidmos MA, Dayal MR. "Sex determination from the talus of South African whites by discriminant function analysis", Am J Forensic Med & Pathol 2003;24:322–8.

[17] Bidmos MA, Dayal MR. "Further evidence to show population specificity of discriminant function equations for sex determination using the talus of South African blacks", J Forensic Sci. 2004;49(6):1165–70.

[18] DiBernnardo R, Taylor JV. "Sex assessment of the femur: A test of a new method", Am J Phys Anthropol 1979;50:635–8.

[19] Iscan MY, Yoshino M, Kato S. "Sex determination from the tibia: Standards for Contemporary Japan" J Forensic Sci 1994;39:785–92.

[20] SteynM, ˙Iscan MY. "Sex determination from the femur and tibia in South African whites", Forensic Sci Int 1997;90:111–9.

[21] King CA, ˙Iscan MY, Loth SR. "Metric and comparative analysis of sexual dimorphism in the Thai femur", J Forensic Sci 1998;43:954–8.

[22] Bidmos MA, Asala SA. "Discriminant function sexing of the calcaneus of the South African whites", J Forensic Sci 2003;48:1213–8.

[23] Bidmos MA, Asala SA. "Sexual dimorphism of the calcaneus of South African blacks", J Forensic Sci 2004;49:446–50.

[24] Asala SA, Bidmos MA, Dayal MR. "Discriminant function sexing of fragmentary femur of South African blacks", Forensic Sci Int 2004; 145:25–9.

[25] Black TK. "A new method for assessing the sex of fragmentary skeletal remains: femoral shaft circumference", Am J Phys Anthropol 1978;48:227–32.

[26] Kieser JA, Moggi–Cecchi J, Groeneveld HT. "Sex allocation of skeletal material by analyses of the proximal tibia", Forensic Sci Int 1992;56:29–36.

[27] Asala SA, Mbajiorgu FE, Papandro BA. "A comparative study of femoral head diameters and sex differentiation in Nigerians", Acta Anatomica 1998;162:232–7.

[28] Asala SA. "Sex determination from the head of the femur of South African whites and blacks", Forensic Sci Int 2001;117:15–22.

[29] Asala SA. “The efficiency of the demarking point of the femoral head as a sex determining parameter”, Forensic Sci Int 2002;127:114–8.
[30] Loth SR, ˙Iscan MY. “Sex determination”, In: Siegel J, Saukko PJ, Knupfer GC, editors. Encyclopedia of forensic sciences. Vol 1. San Diego, CA:Academic Press, 2000;252–60.
[31] Williams PL. “Gray’s anatomy: the anatomical basis of medicine and Surgery”, 38th ed. Edinburgh: Churchill Livingstone, 1995.
[32] Introna Jr F, Di Vella G, Campobasso CP. “Sex determination by discriminant function analysis of patella measurements”, Forensic Sci Int 1998;95:39–45.
[33] Gunn MC, McWilliams KR. “A method for estimating sex of the human skeleton from the volume of the patella, talus, or calcaneus” HOMO 1980;31:189–98.
[34] Bidmos MA, Steinberg N, Kuykendall KL. “Patella measurements of South African whites as sex assessors”, HOMO 2005;56:69–74.
[35] Tatarek N., Lease L., “Further analysis of utilizing the human patella to determine sex in forensic contexts”, Program of the Seventy-First Annual Meeting of the American Association of Physical Anthropologists,153, 2002.
[36] Ariane Kemkes-Grottenthaler, “Sex determination by discriminant analysis: an evaluation of the reliability of patella measurements”, J Forensic Sci 2005;147:129-133.
[37] Dayal MR., Bidmos MA., “Discriminating sex in south African blacks using patella dimensions”, J Forensic Sci, Nov. 2005;150, 6.
[38] O’Connor W.G., “The dimorphic sesamoid: differentiating the patella of females and males by height, width and thickness measurements”, Master’s thesis of Arts in Department of Anthropology-university of South Carolina, 1996.
[39] MY Iscan, “Forensic anthropology of sex and body size”, Forensic science International Journal, 147:107-112, 2005.
[40] Y. M. Kadah, Aly A. Farag, Jacek M. Zurada , A. M. Badawi, Abou-Bakr M. Youssef, “Classification Algorithms for Quantitative Tissue Characterization of Diffuse Liver Disease from Ultrasound Images”, IEEE Transaction on Medical Imaging Journal, August, 1996;15,4:466-478.
[41] Ahmed M. Badawi, Ahmed S. Derbala and Abou-Bakr M. Youssef, "Fuzzy logic algorithm for quantitative tissue characterization of diffuse liver diseases from ultrasound images," International Journal of Medical Informatics 55-2 pp. 135-147, 1999.
[42] Bassem S. Wadie, Ahmed M. Badawi, and Mohamed A Ghoneim “The Relationship of International Prostate Symptom Score and Objective Parameters for Diagnosing Bladder Outlet Obstruction: Part II: The Potential Usefulness of Artificial Neural Networks”, American Journal of Urology, Vol. 165, 35-37, January 2001.
[43] Ahmed M. Badawi, Manal Abdel-Wahed, Bassem S. Wadie, and Shimaa Imbaby, "Diagnosis of Bladder Outlet Obstruction By Quantitative Features Using Neural Networks", Ain Shams 2nd International Conference on Electronics, Circuits & Systems, 347-349, 2004.
[44] Ahmed M. Badawi, Kahled G. Hasan, Emam-Elhak A. Aly, and Rimon A. Messiha, "Chromosomes Classification Based on Neural Networks, Fuzzy Rule Based, and Template Matching Classifiers," In Proceedings of The 46th IEEE International Midwest Symposium on Circuits and Systems (MWSCAS), 2003.
[45] Lorenz C., Krahnstoever N., “Generation of Point-Based 3D Statistical Shape Models for Anatomical Objects,”/ Computer Vision and Image Understanding, (77): 175-181,2000.
[46] P. J. Besl and N. McKay. A method for registration of 3-D shapes. *IEEE PAMI*, 14(2):239–256, Mar 1992.
[47] Merkl B., Mahfouz M., “Unsupervised Three-Dimensional Segmentation of Medical Images Using an Anatomical Bone Atlas,” 12th International Conference on Biomedical Engineering, Singapore, 2005.